Appendix-A

(TABS-MD model results for low and high flow conditions)

The results of model simulation for low flow conditions:

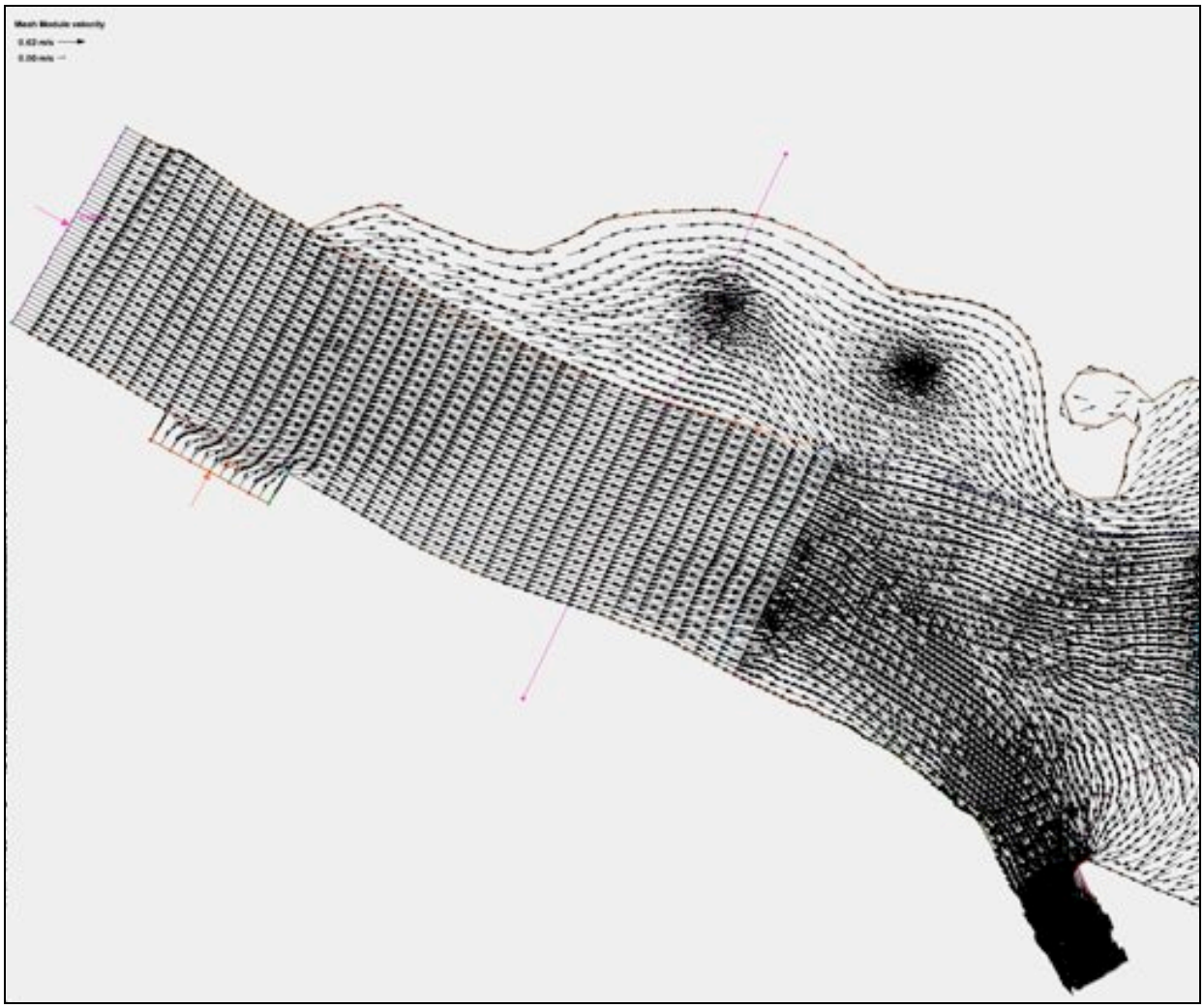

Fig. A1a. Velocity vectors predicted by the model for the upper part of the computational domain for low flow condition.

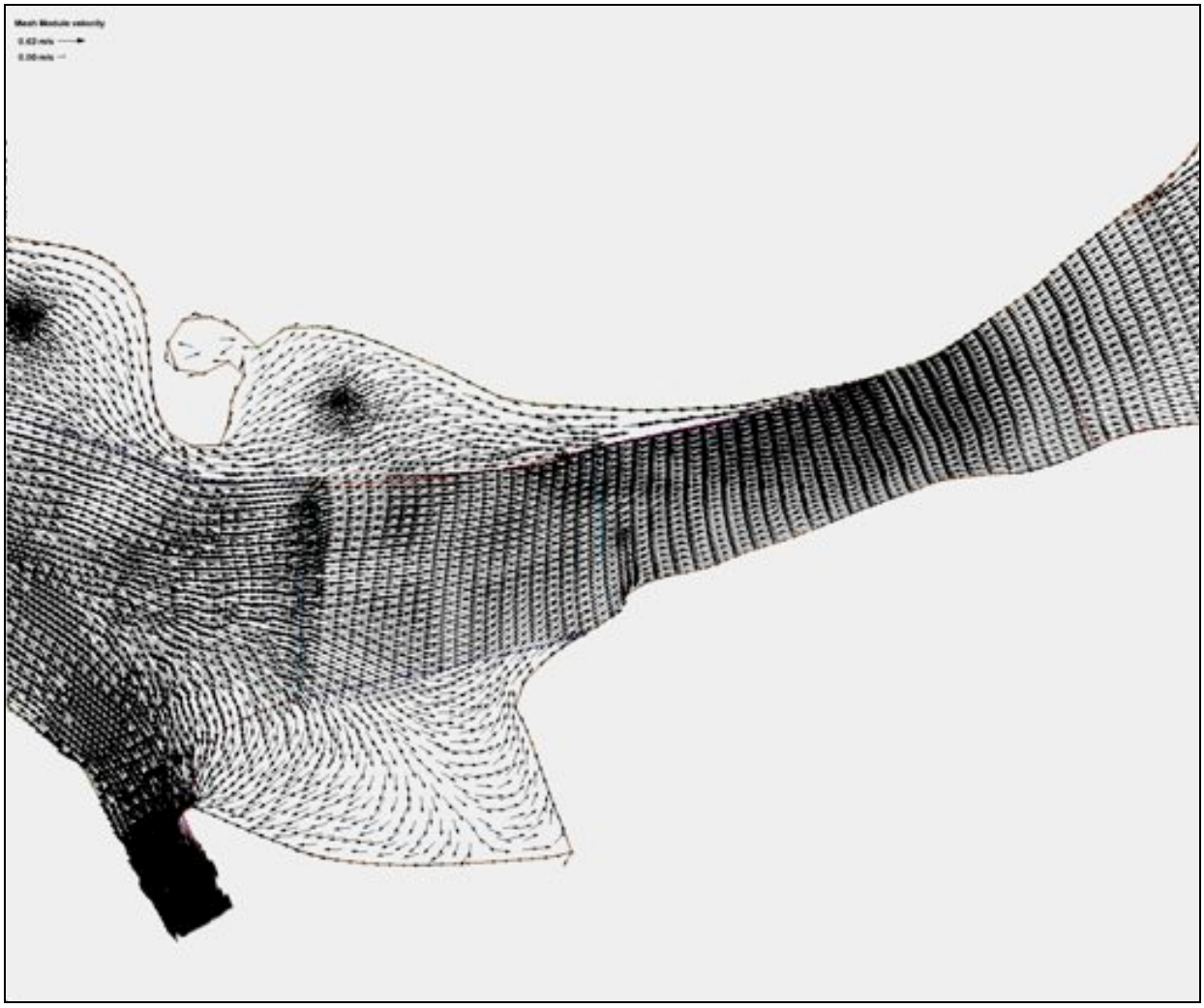

Fig. A1b. Velocity vectors predicted by the model for the middle part of the computational domain for low flow condition.

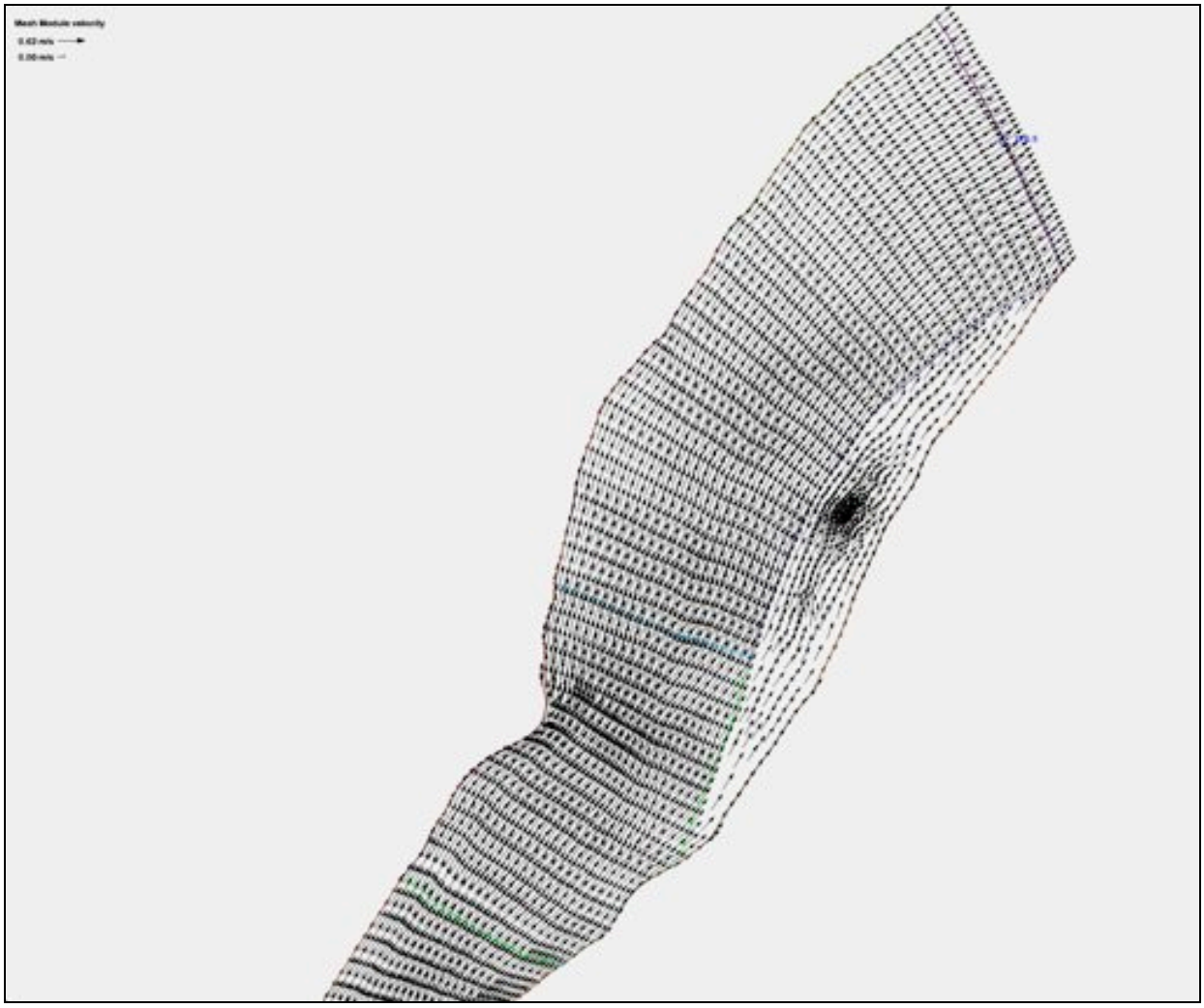

Fig. A1c. Velocity vectors predicted by the model for the lower part of the computational domain for low flow condition.

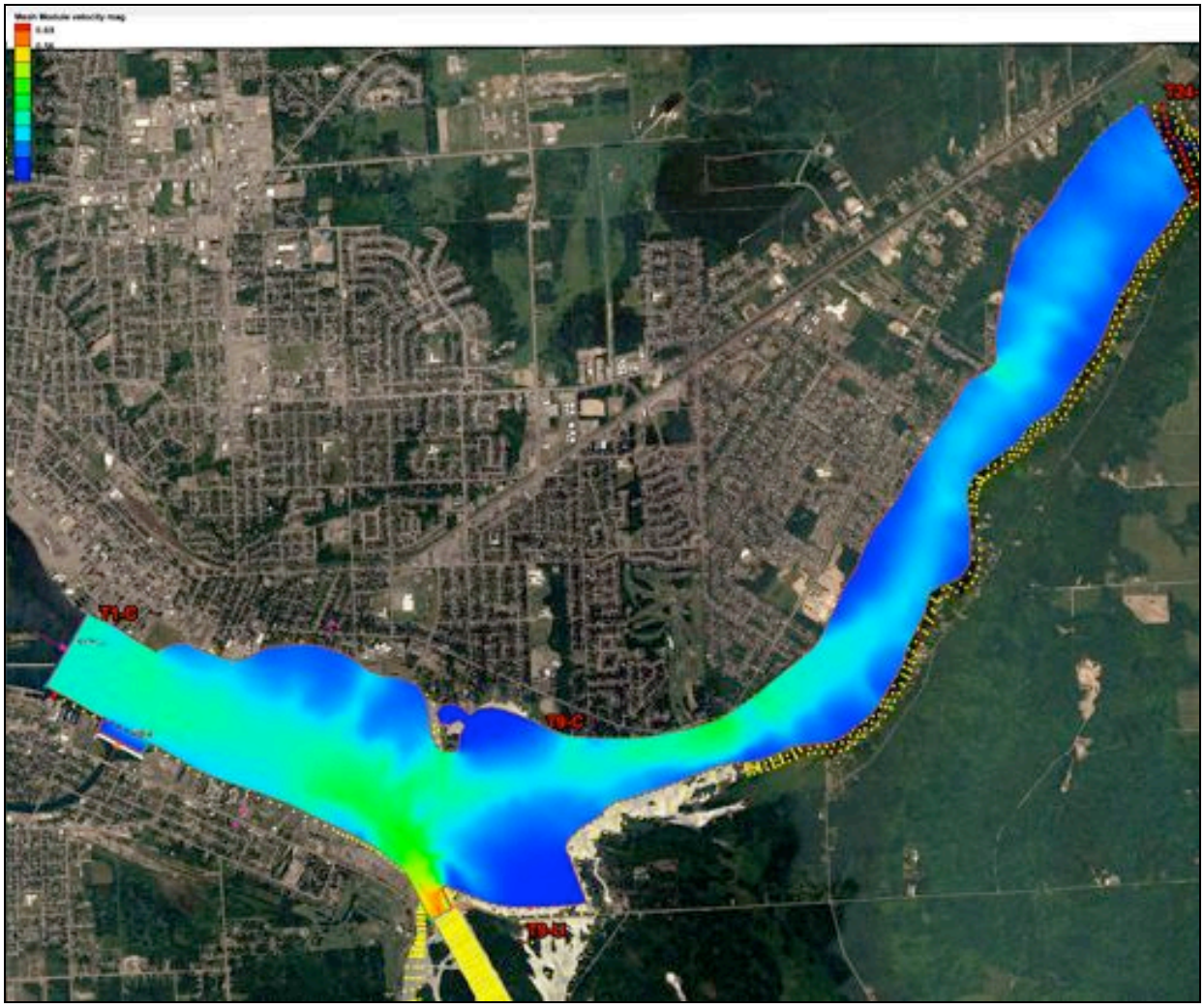

Fig. A2. Distribution of velocity magnitude predicted by the model for the low flow condition.

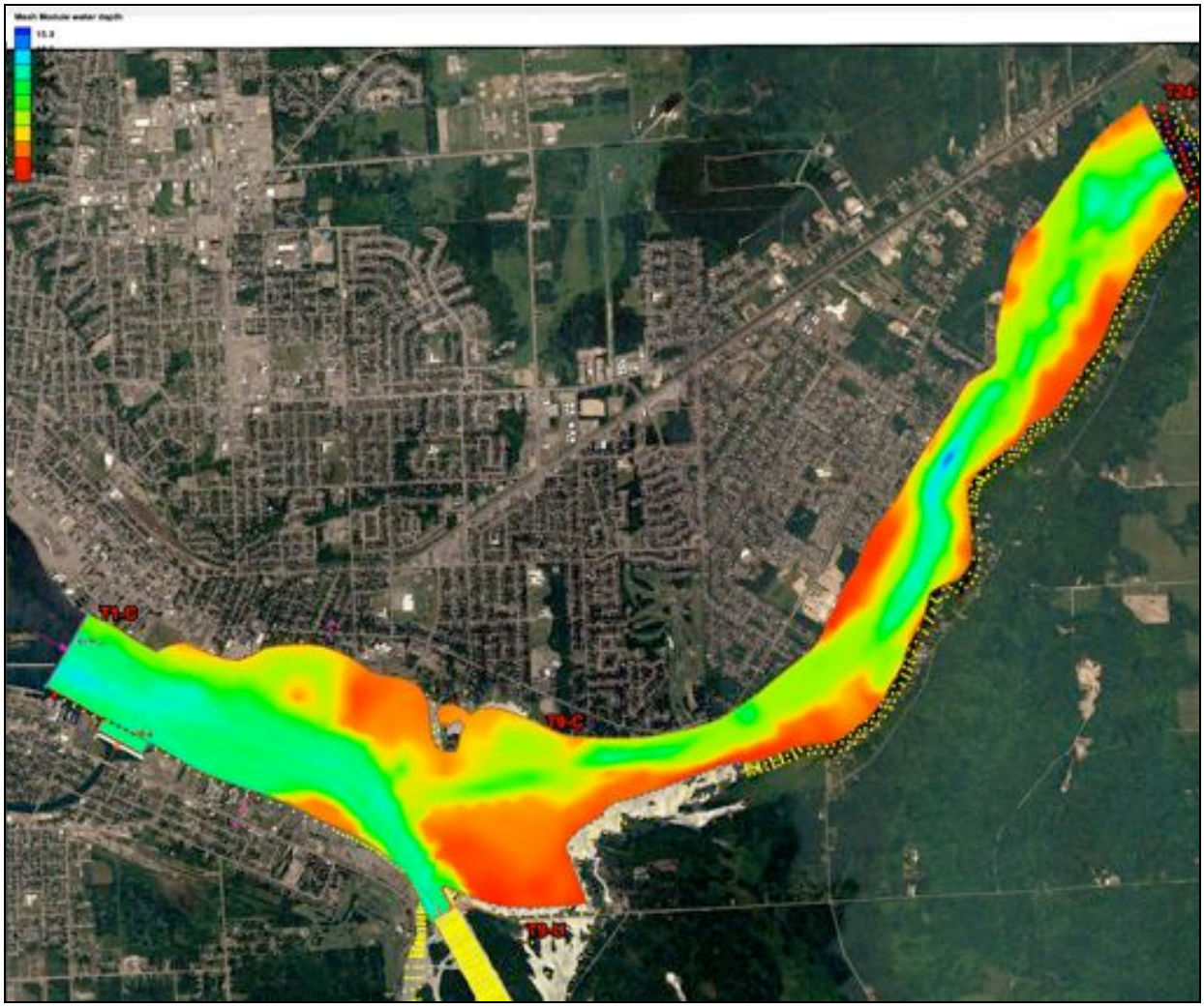

Fig. A3. Distribution of water depth predicted by the model for the low flow condition.

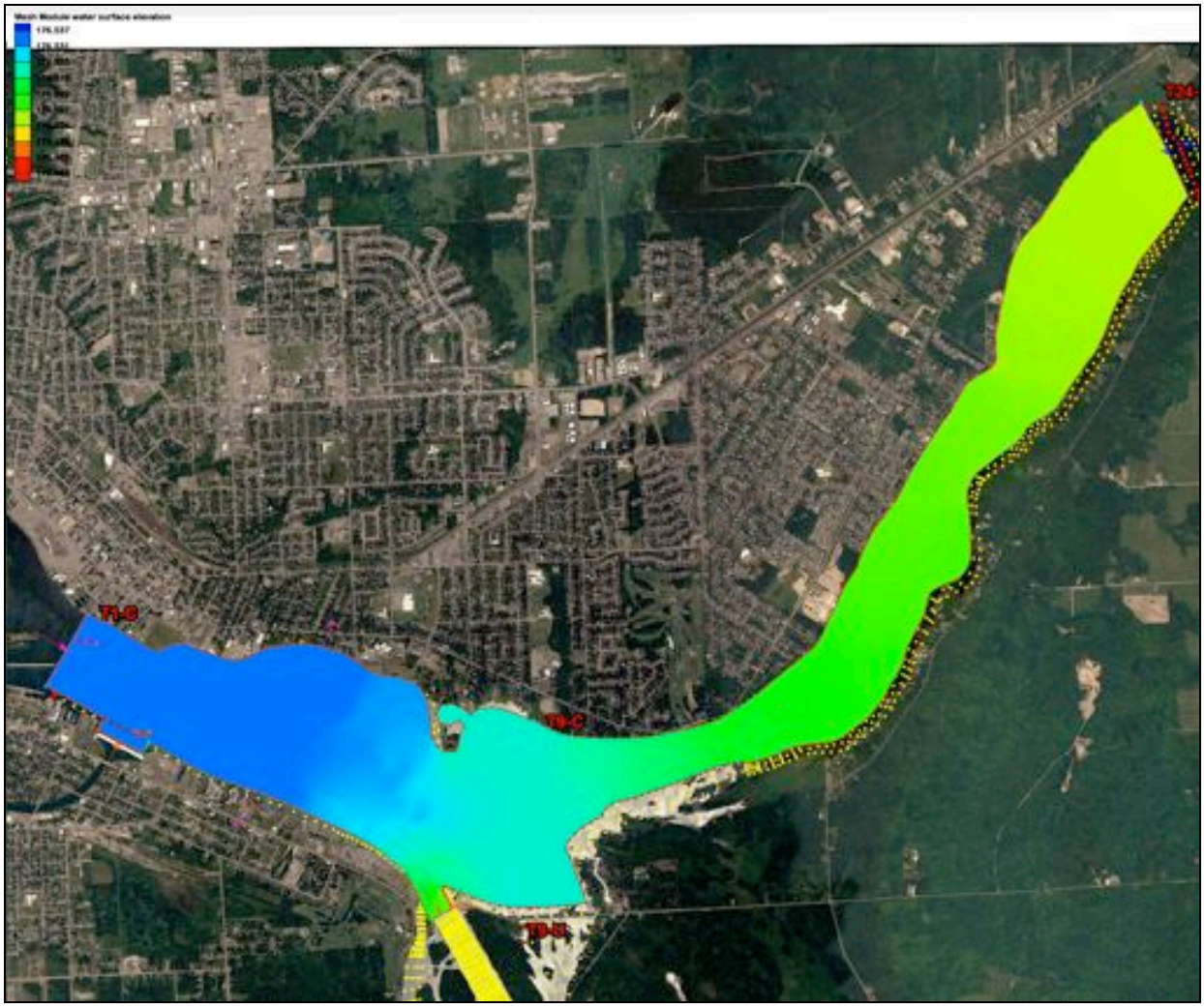

Fig.A4 Distribution of water surface elevation predicted by the model for low flow condition.

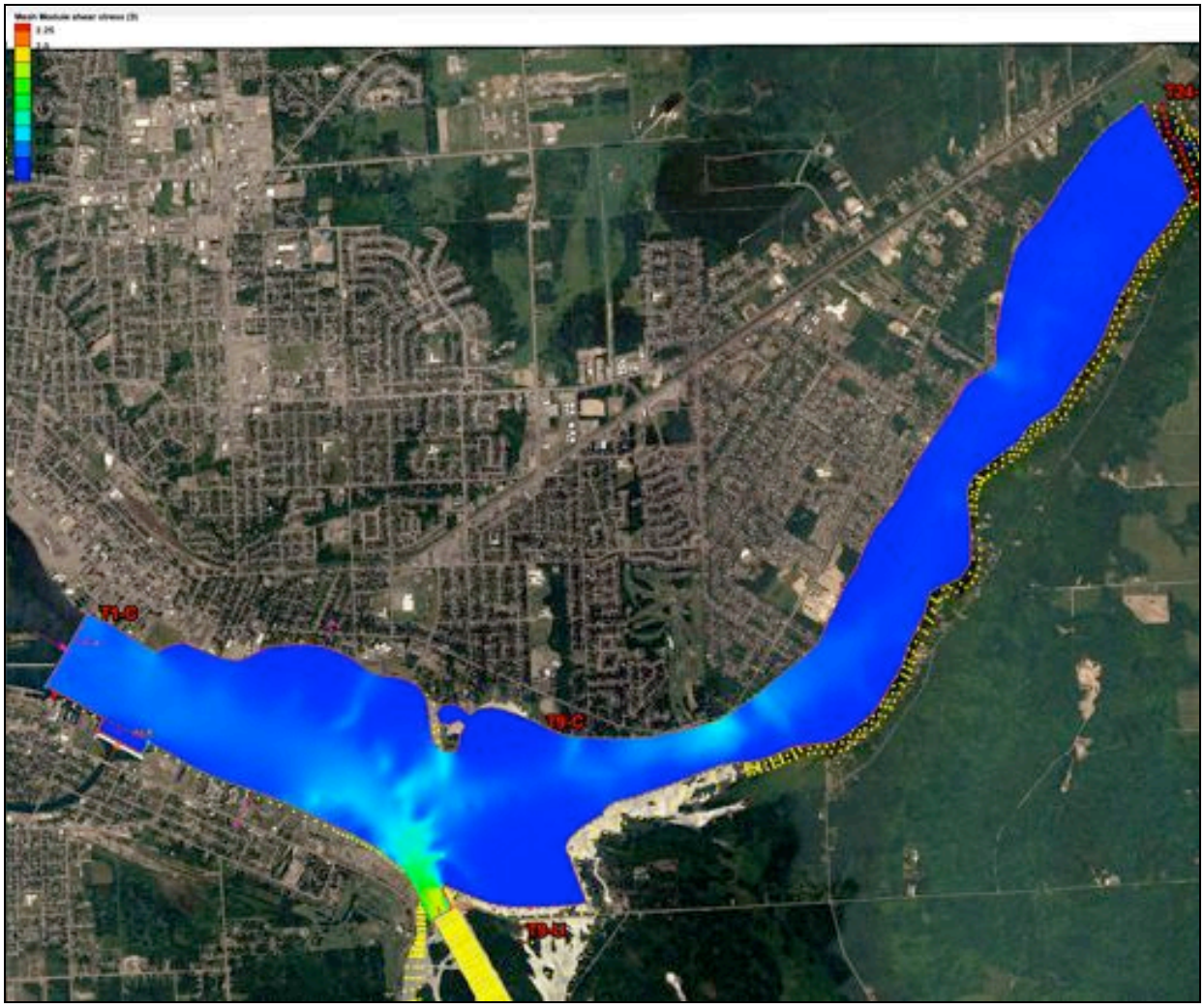

Fig.A5. Distribution of bed shear stress predicted by the model for low flow condition.

Predicted flow properties for high flow condition.

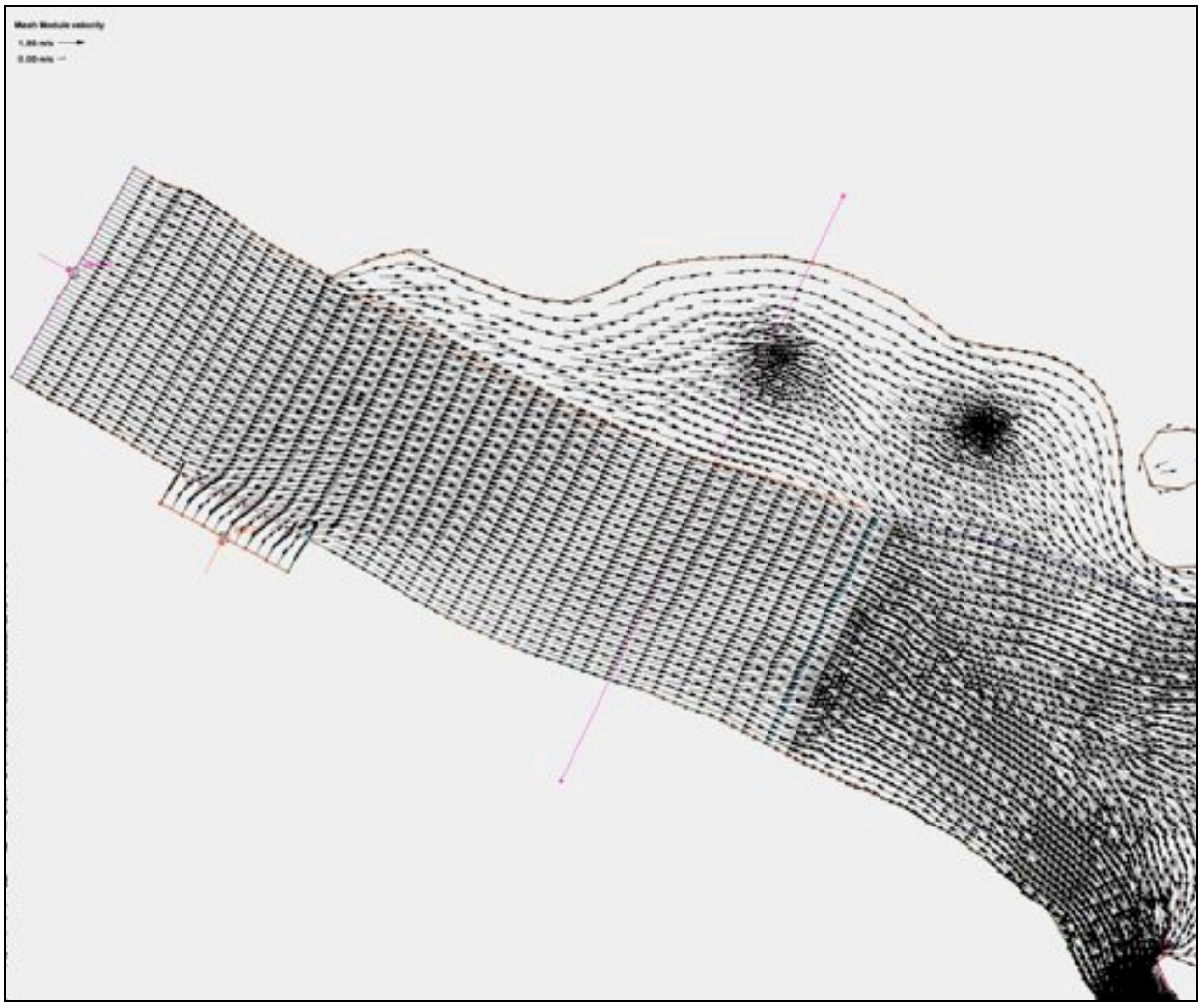

Fig. A6a. Predicted velocity vectors in the upper part of the computational domain for the high flow condition.

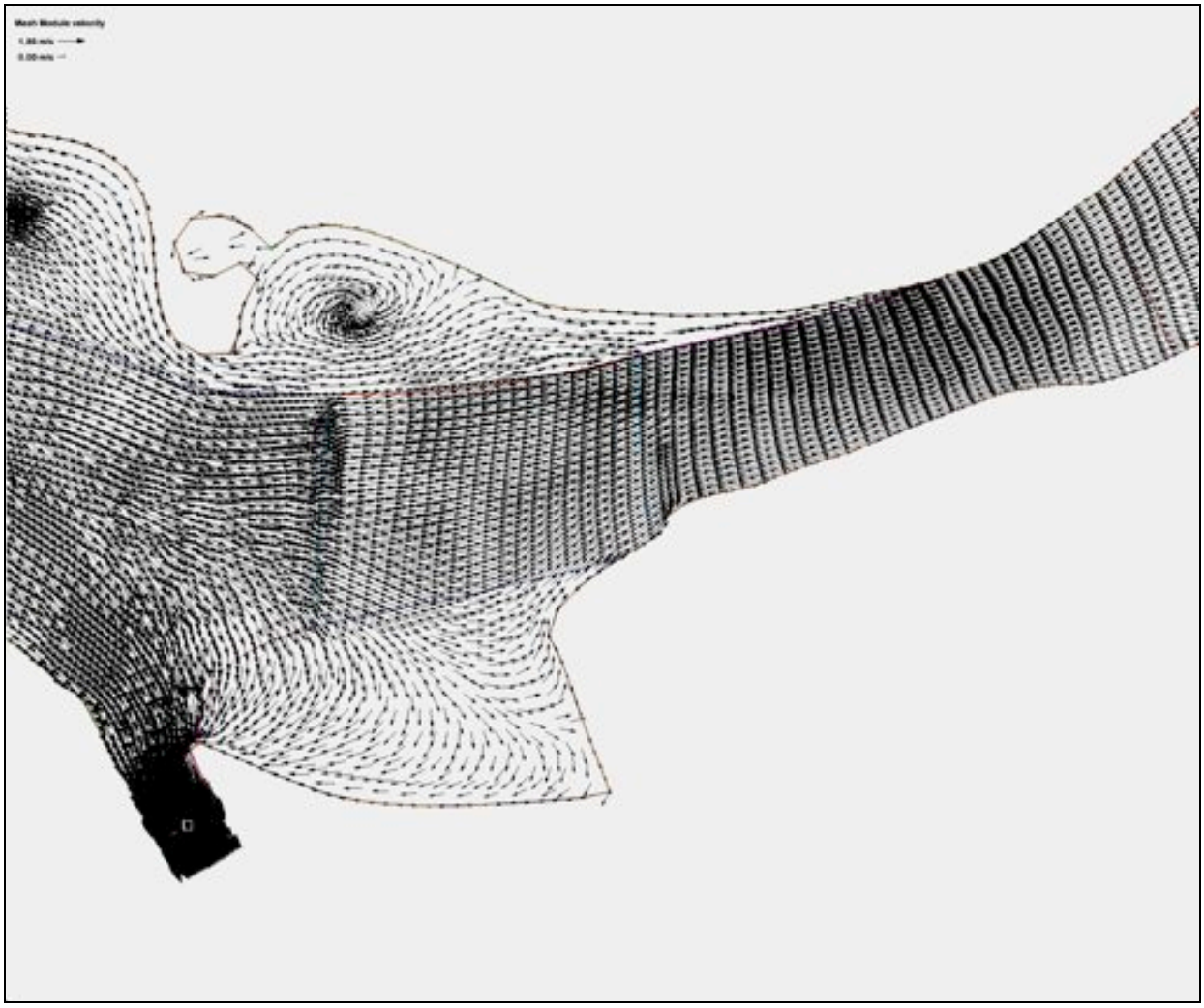

Fig. A6b. Predicted velocity vectors in the middle part of the computational domain for the high flow condition.

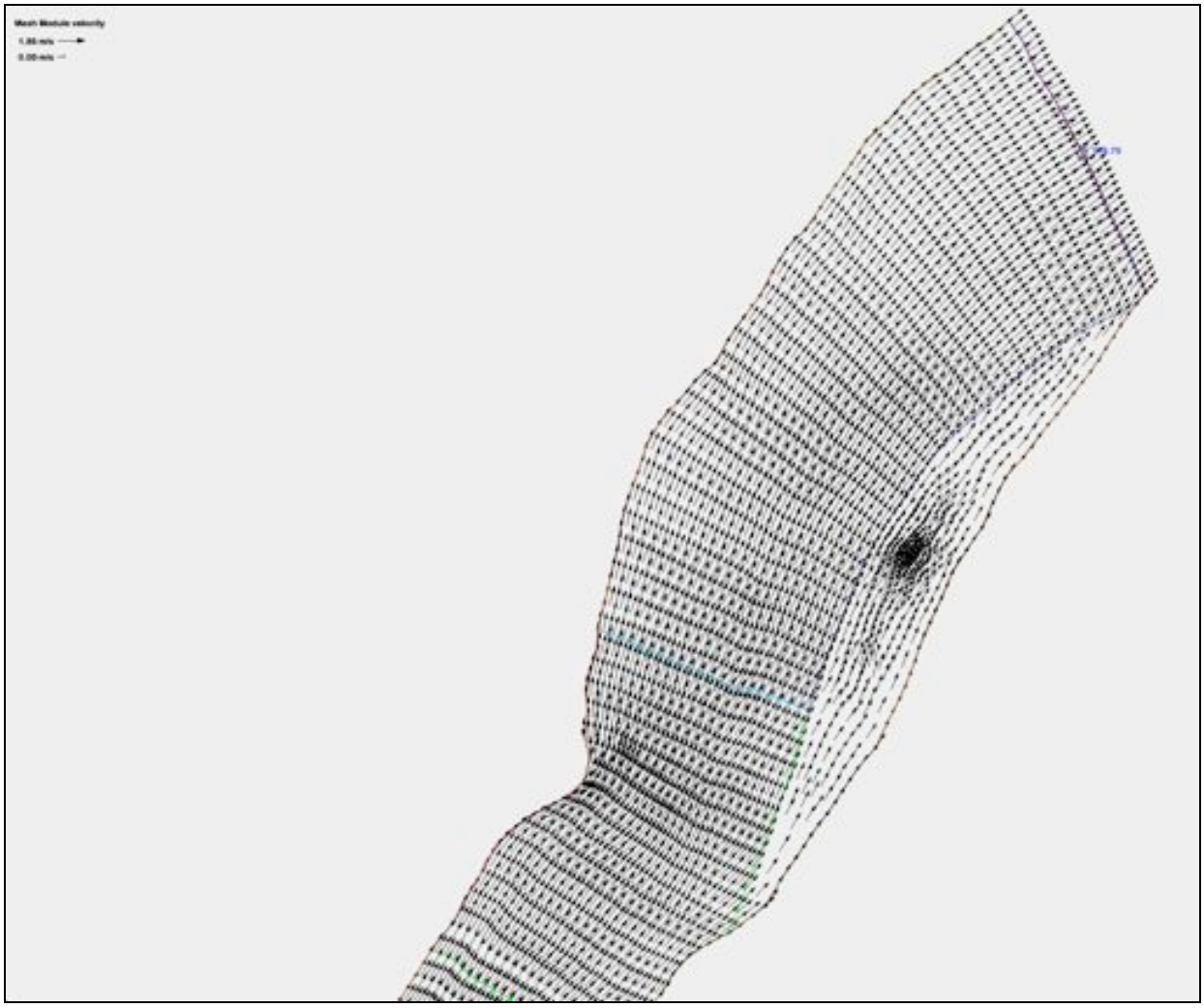

Fig. A6c. Predicted velocity vectors in the lower part of the computational domain for the high flow condition.

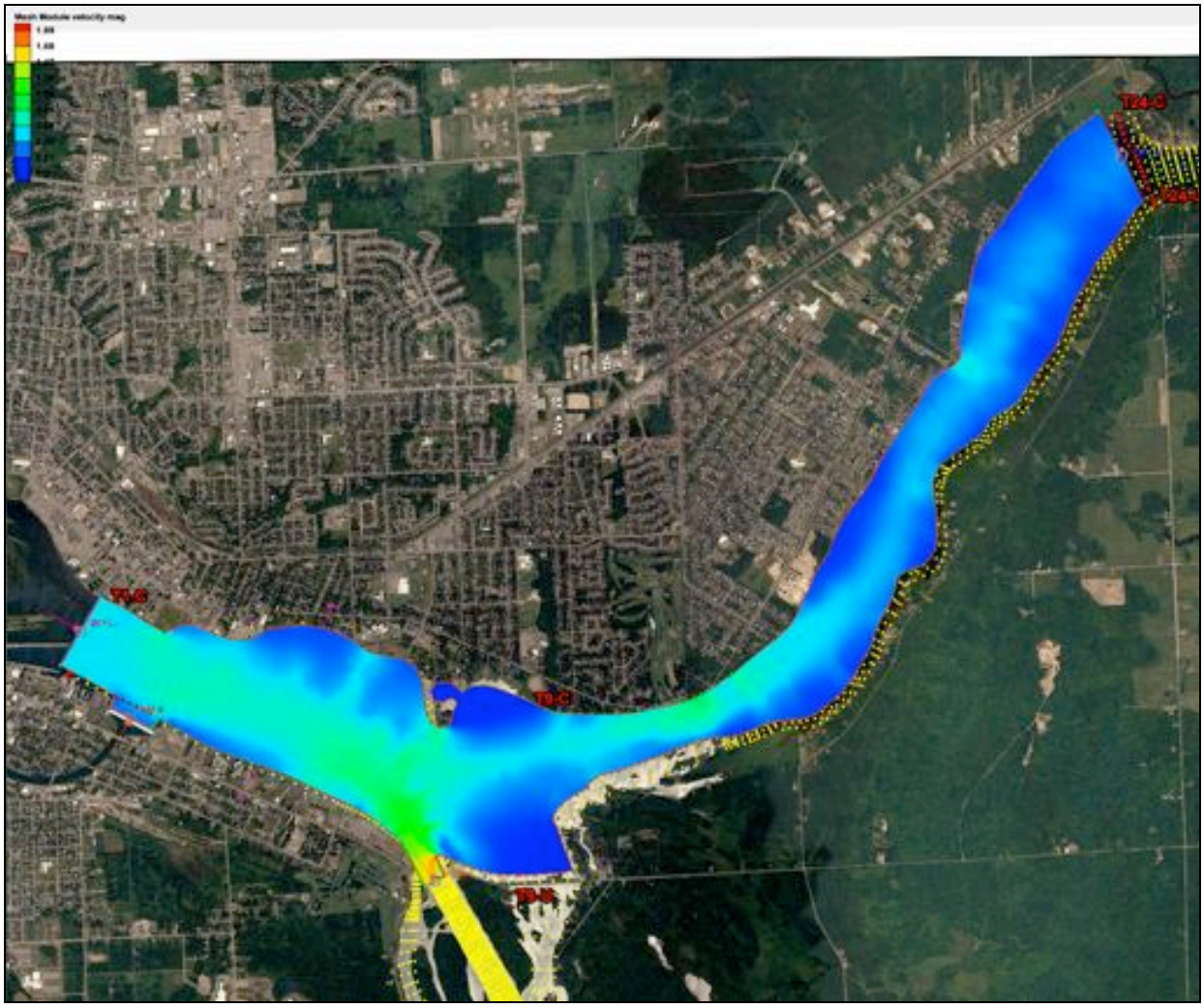

Fig. A7. Predicted velocity magnitudes by the model for the high flow condition.

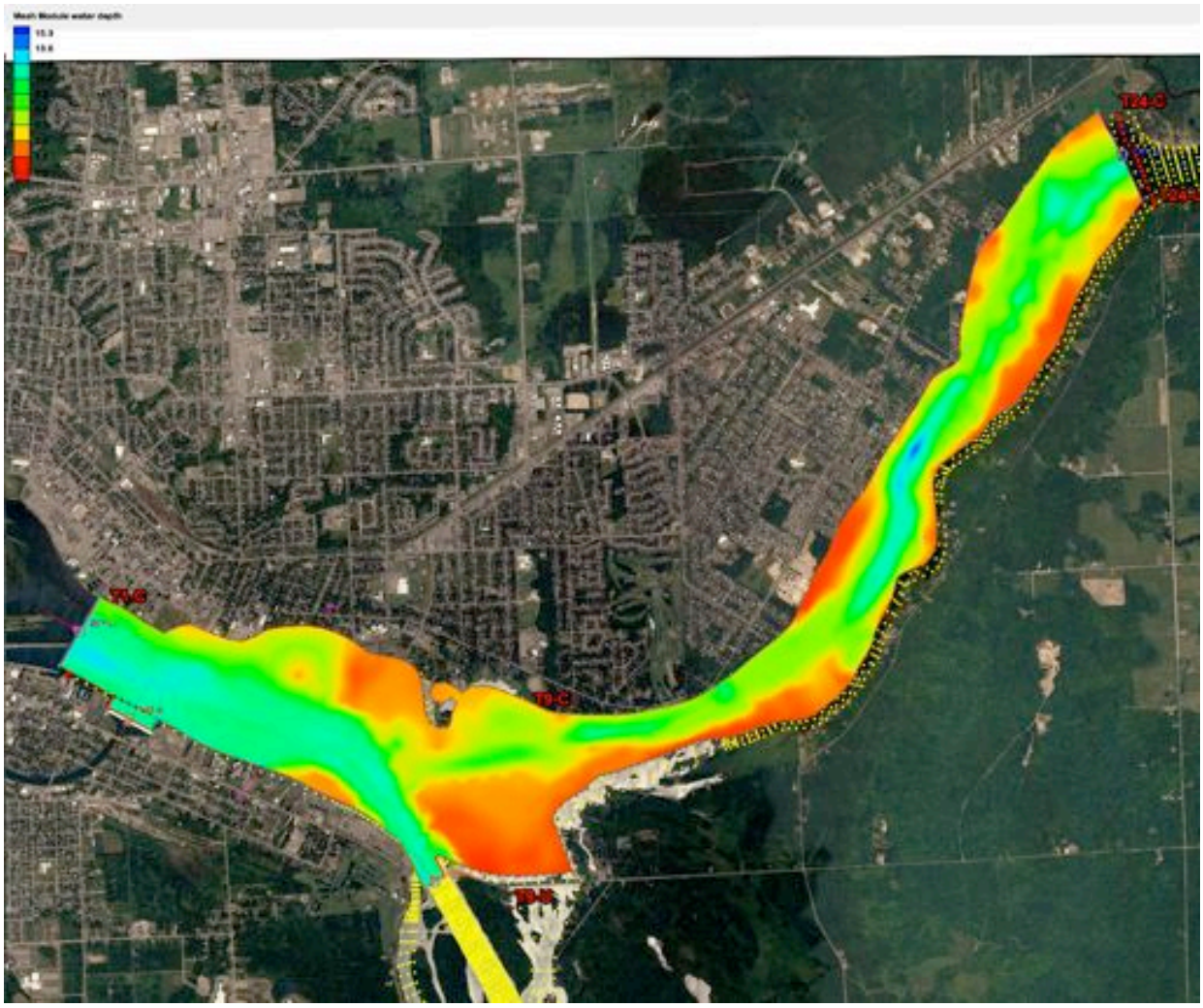

Fig. A8. Predicted flow depth distribution for the high flow condition.

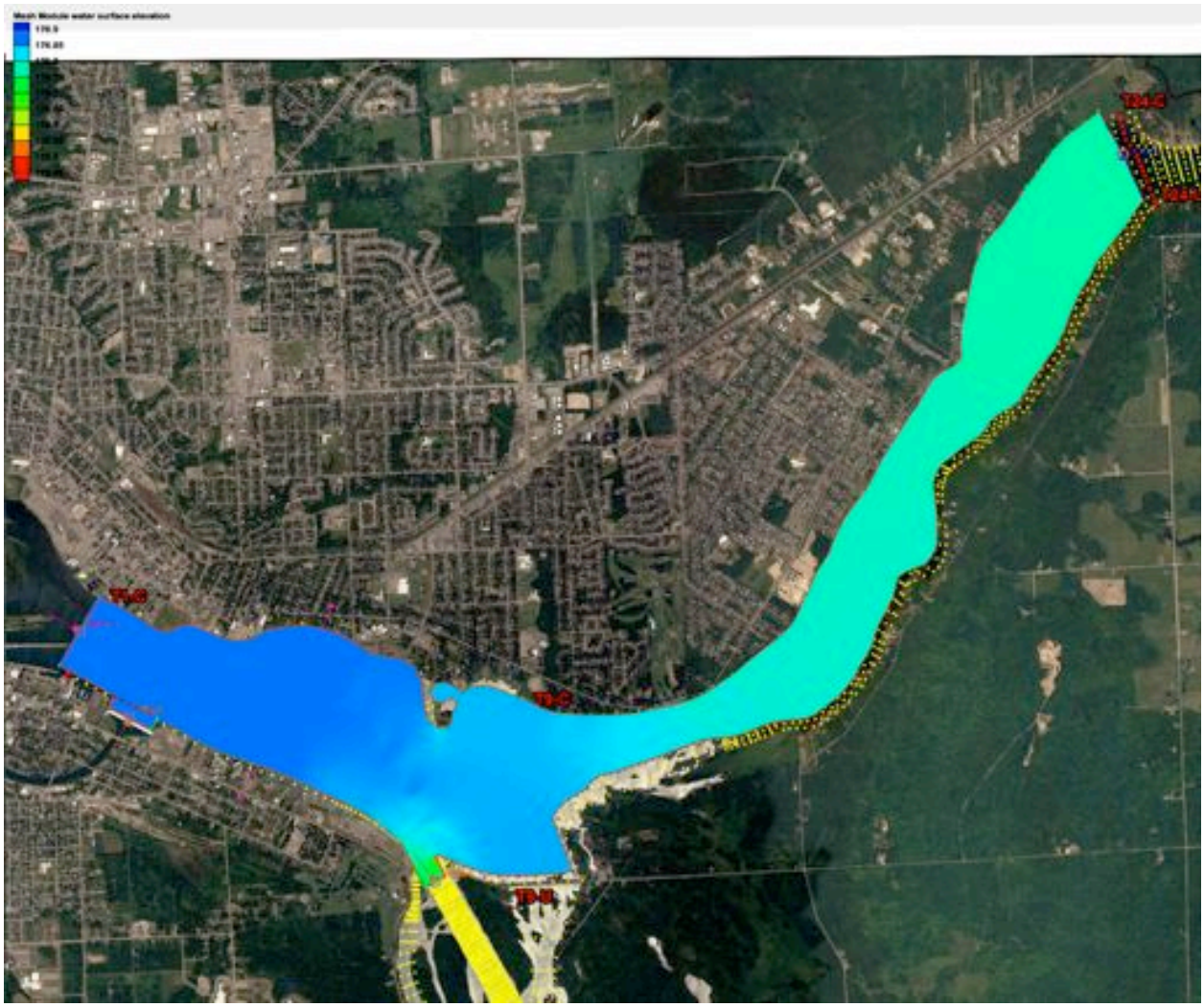

Fig. A9. Predicted water surface elevation by the model for the high flow condition.

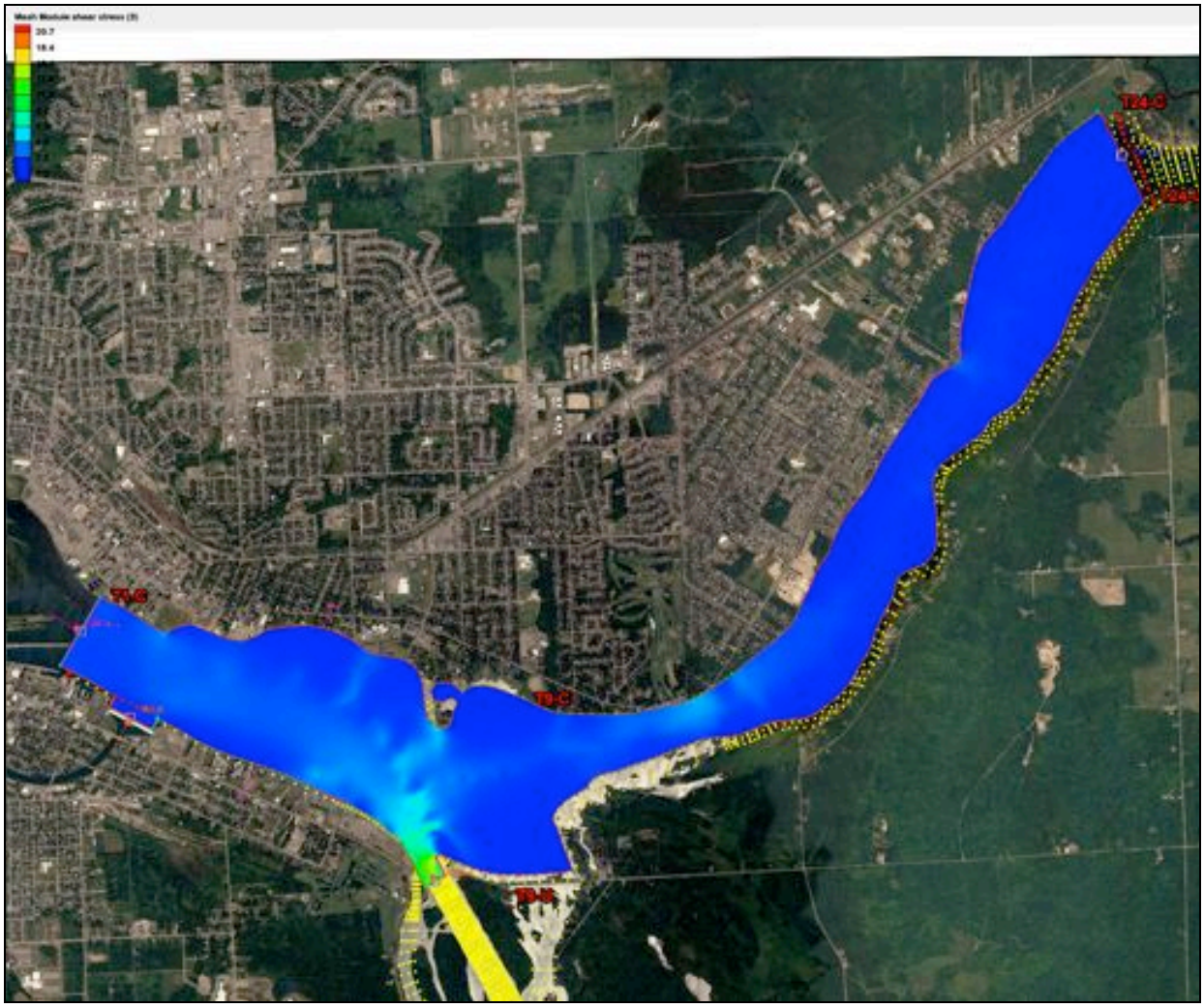

Fig. A10. Predicted bed shear stress distributions for the high flow condition.

APPENDIX-B

(Photographs of the grab samples)

Fig. B1. Photograph of grab sample collected at Transect 2 (Sample id: SMR-T2-2).

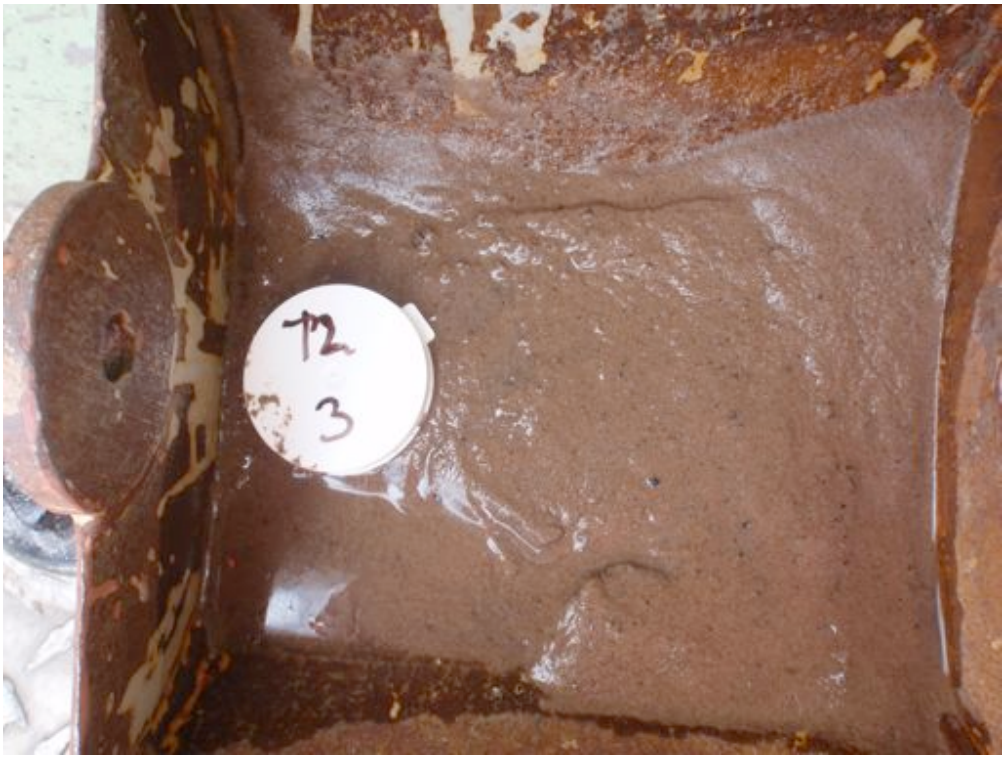

Fig. B2. Photograph of the grab sample collected at Transect 2 (Sample id: SMR- T2-3).

Fig.B3. Photograph of the grab sample collected at Transect 3 (Sample id: SMR-T3-1).

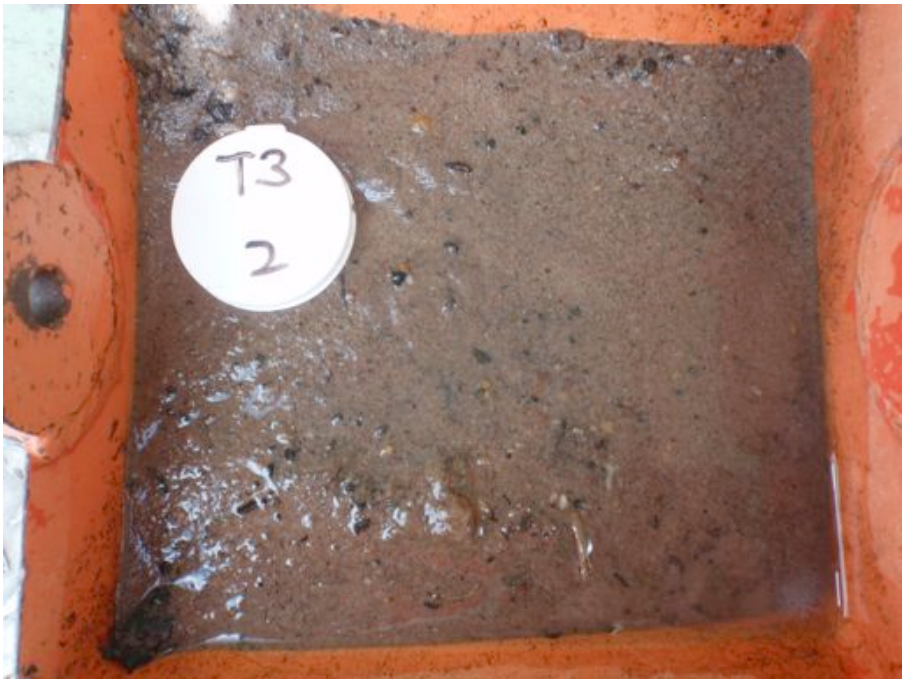

Fig. B4. Photograph of the grab sample collected at Transect 3 (Sample id: SMR-T3-2).

Fig. B5. Photograph of the grab sample collected at Transect 3 (Sample id: SMR-T3-3).

Fig. B6. Photograph of the grab sample collected at Transect 4 (Sample id: SMR-T4-1).

Fig. B7. Photograph of the grab sample collected at Transect 4 (Sample id: SMR-T4-2).

Fig. B8. Photograph of the grab sample collected at Transect 4 (Sample id: SMR-T4-3).

Fig. B9. Photograph of the grab sample collected at Transect 5 (Sample id: SMR-T5-1).

Fig.B10. Photograph of the grab sample collected at Transect 9 (Sample id: SMR-T9-1).

Fig. B11. Photograph of the grab sample collected at Transect 9 (Sample id: SMR-T9-2).

Fig. B12. Photograph of the grab sample collected at Transect 10 (Sample id: SMR-T10-1).

Fig. B13. Photograph of the grab sample collected at Transect 10 (Sample id: SMR-T10-2).

Fig. B14. Photograph of the grab sample collected at Transect 10 (Sample id: SMR-T10-3).

Fig. B15. Photograph of the grab sample collected at Transect 10 (Sample id: SMR-T10-4).

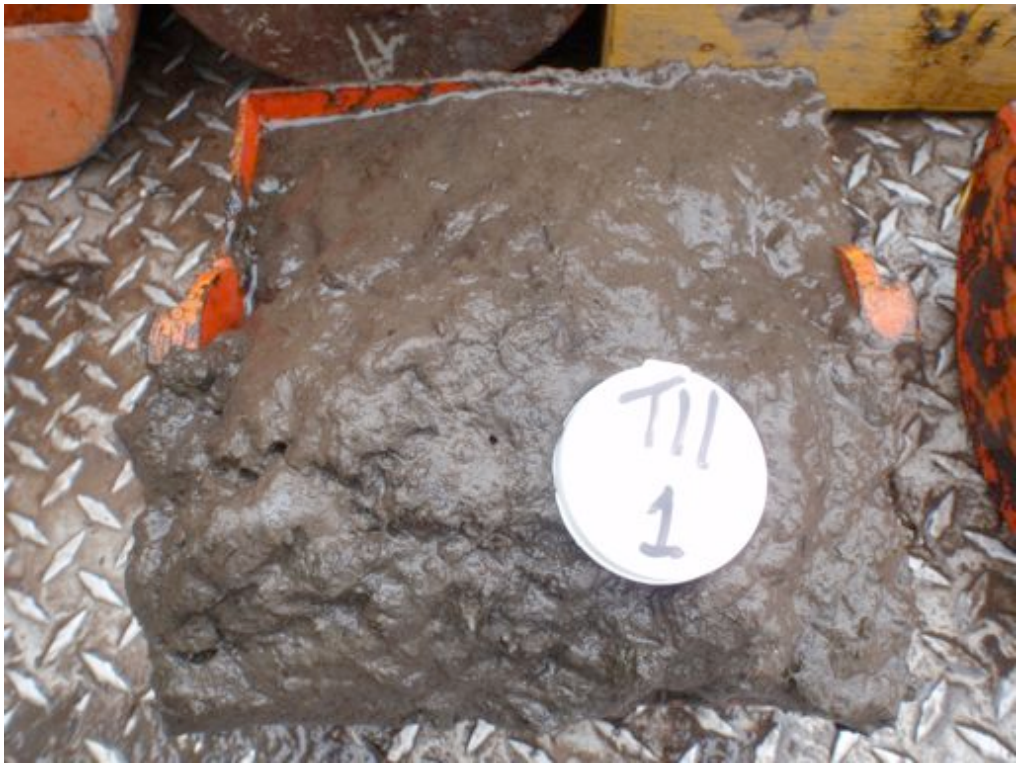

Fig. B16. Photograph of the grab sample collected at Transect 11 (Sample id: SMR-T11-1).

Fig. B17. Photograph of the grab sample collected at Transect 11 (Sample id: SMR-T11-2).

Fig. B18. Photograph of the grab sample collected at Transect 11 (Sample id: SMR-T11-3).

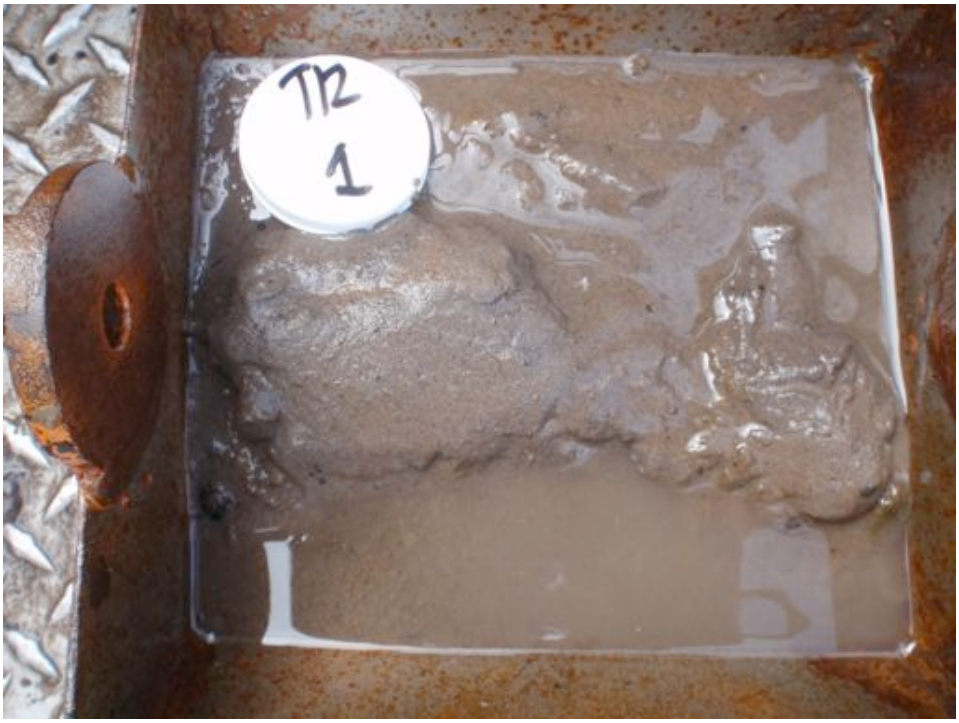

Fig. B19. Photograph of the grab sample collected at Transect 12 (Sample id: SMR-T12-1).

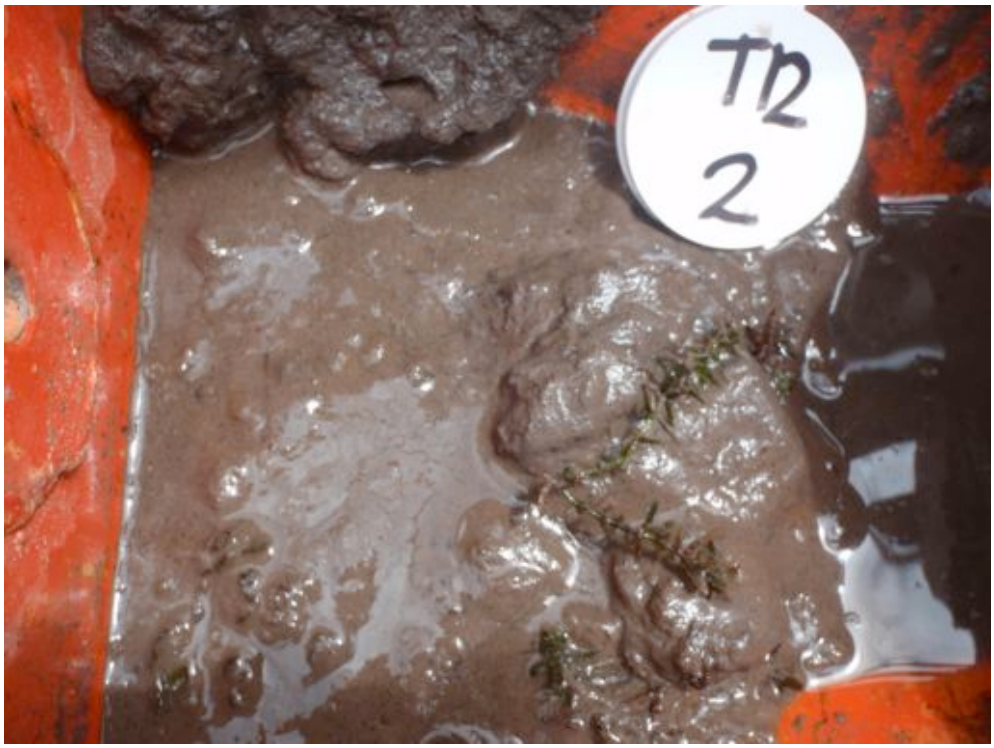

Fig. B20. Photograph of the grab sample collected at Transect 12 (Sample id: SMR-T12-2).

Fig. B21. Photograph of the grab sample collected at Transect 12 (Sample id: SMR-T12-3).

Fig. B22. Photograph of the grab sample collected at Transect 13 (Sample id: SMR-T13-1).

Fig. B23. Photograph of the grab sample collected at Transect 13 (Sample id: SMR-T13-2).

Fig. B24. Photograph of the grab sample collected at Transect 13 (Sample id: SMR-T13-3).

Fig. B25. Photograph of the grab sample collected at Transect 14 (Sample id: SMR-T14-1).

Fig. B26. Photograph of the grab sample collected at Transect 14 (Sample id: SMR-T14-2).

Fig. B27. Photograph of the grab sample collected at Transect 14 (Sample id: SMR-T14-3).

APPENDIX-C

(Simulation of sediment transport in St. Marys River for low and high flows)

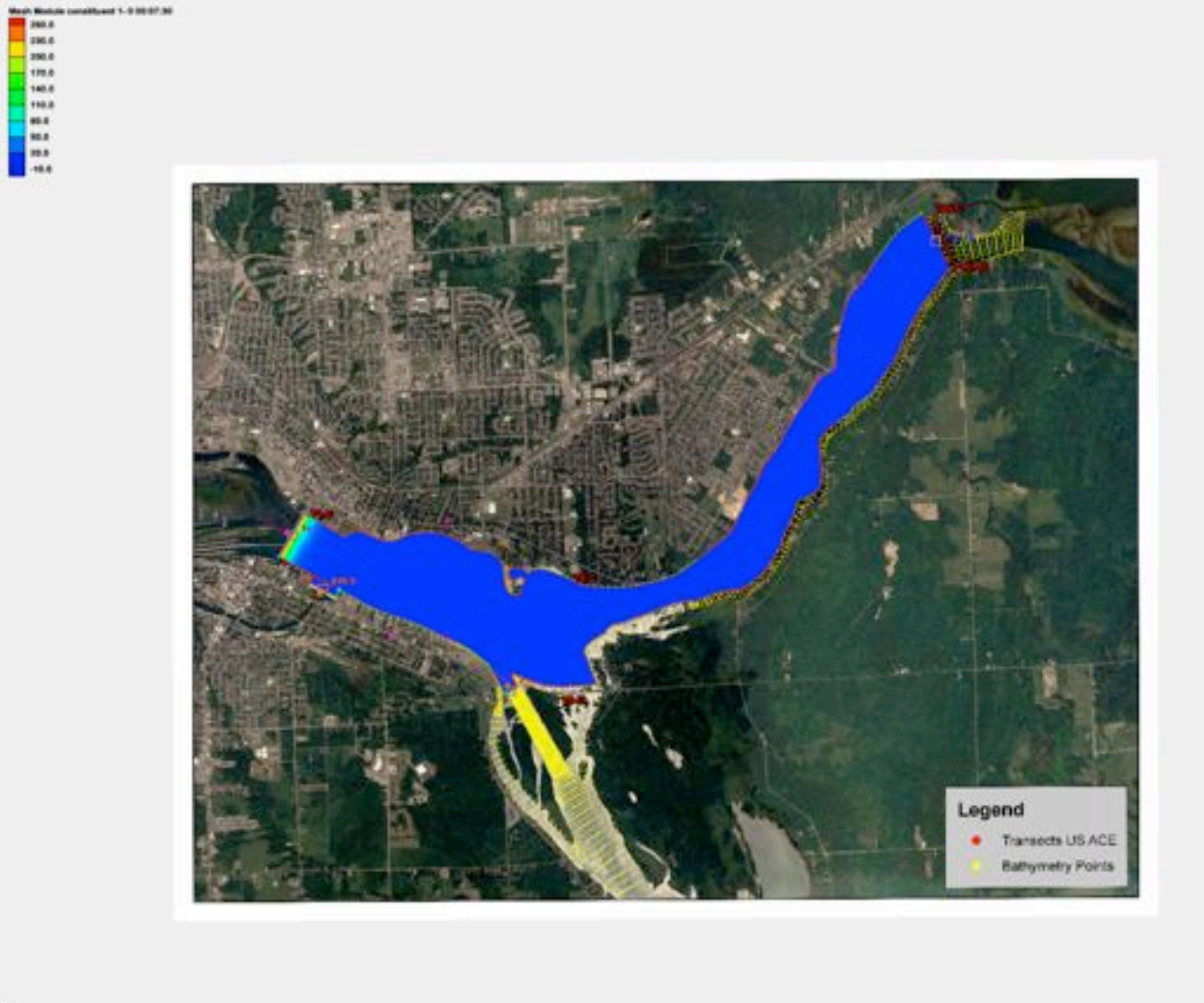

Fig. C1. Simulation of sediment transport in St. Marys River under low flow condition: Elapsed time = 0.125 hrs.

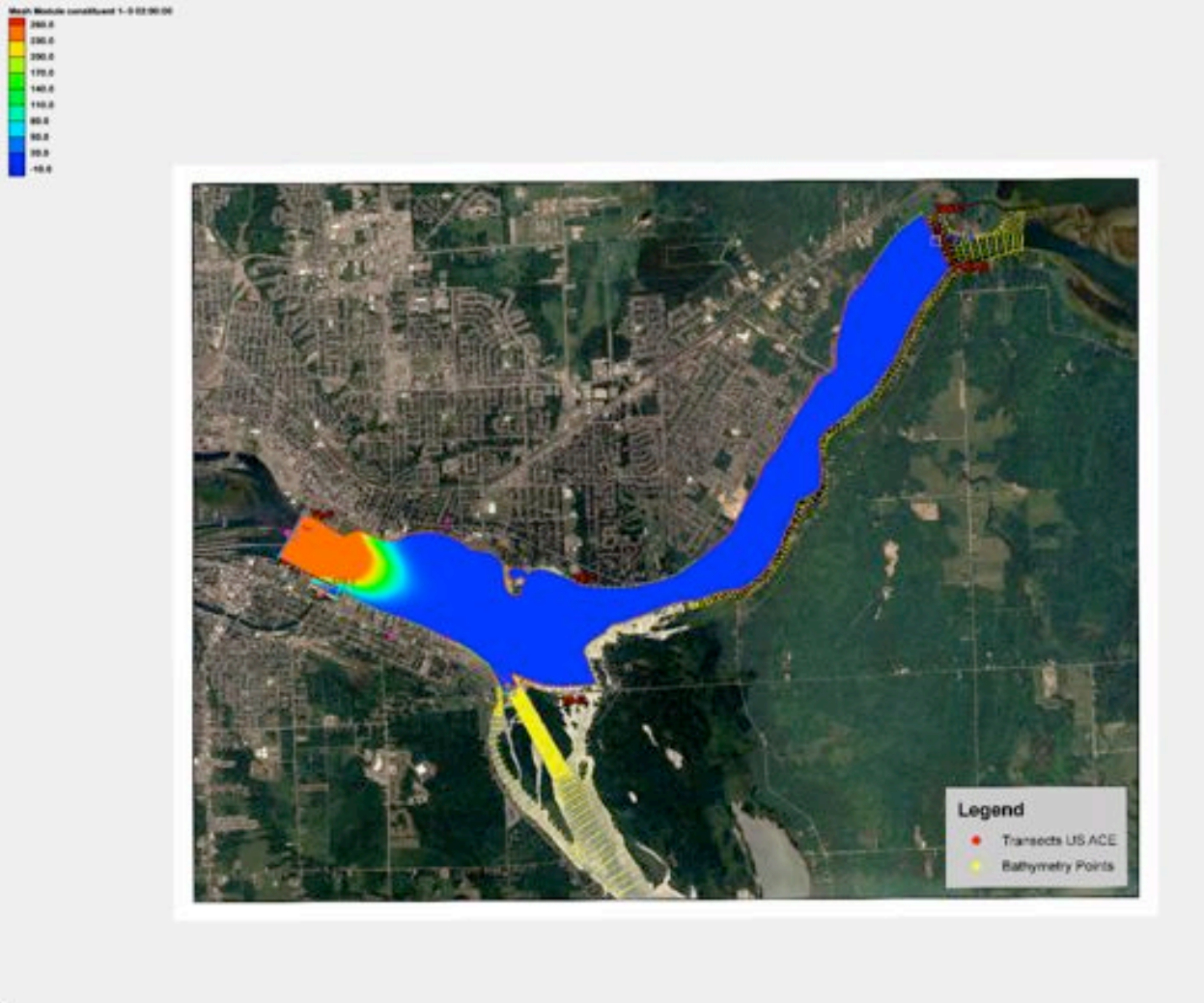

Fig. C2. Simulation of sediment transport in St. Marys River under low flow condition: Elapsed time = 2.0 hrs.

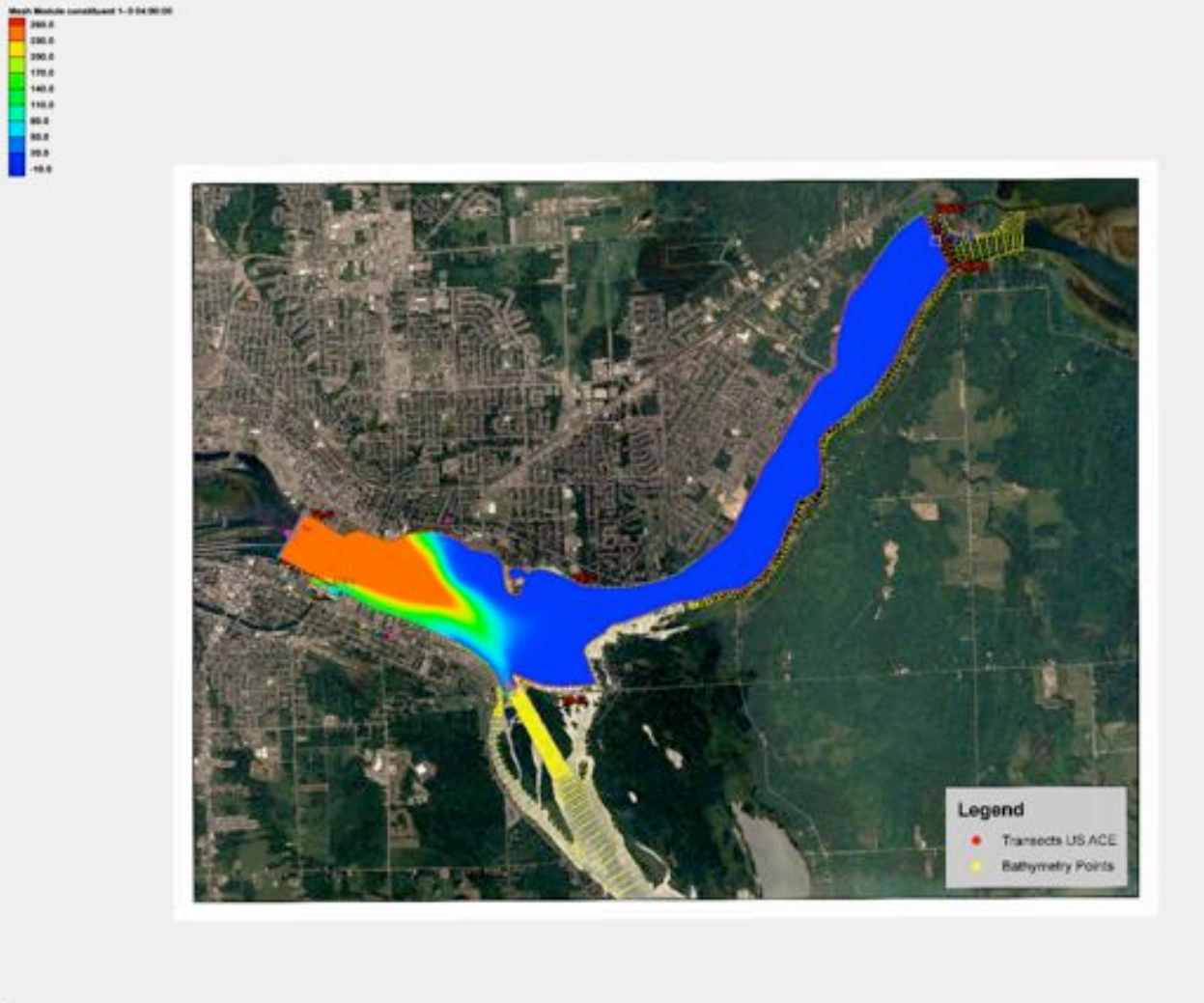

Fig. C3. Simulation of sediment transport in St. Marys River under low flow condition: Elapsed time = 4.0 hrs.

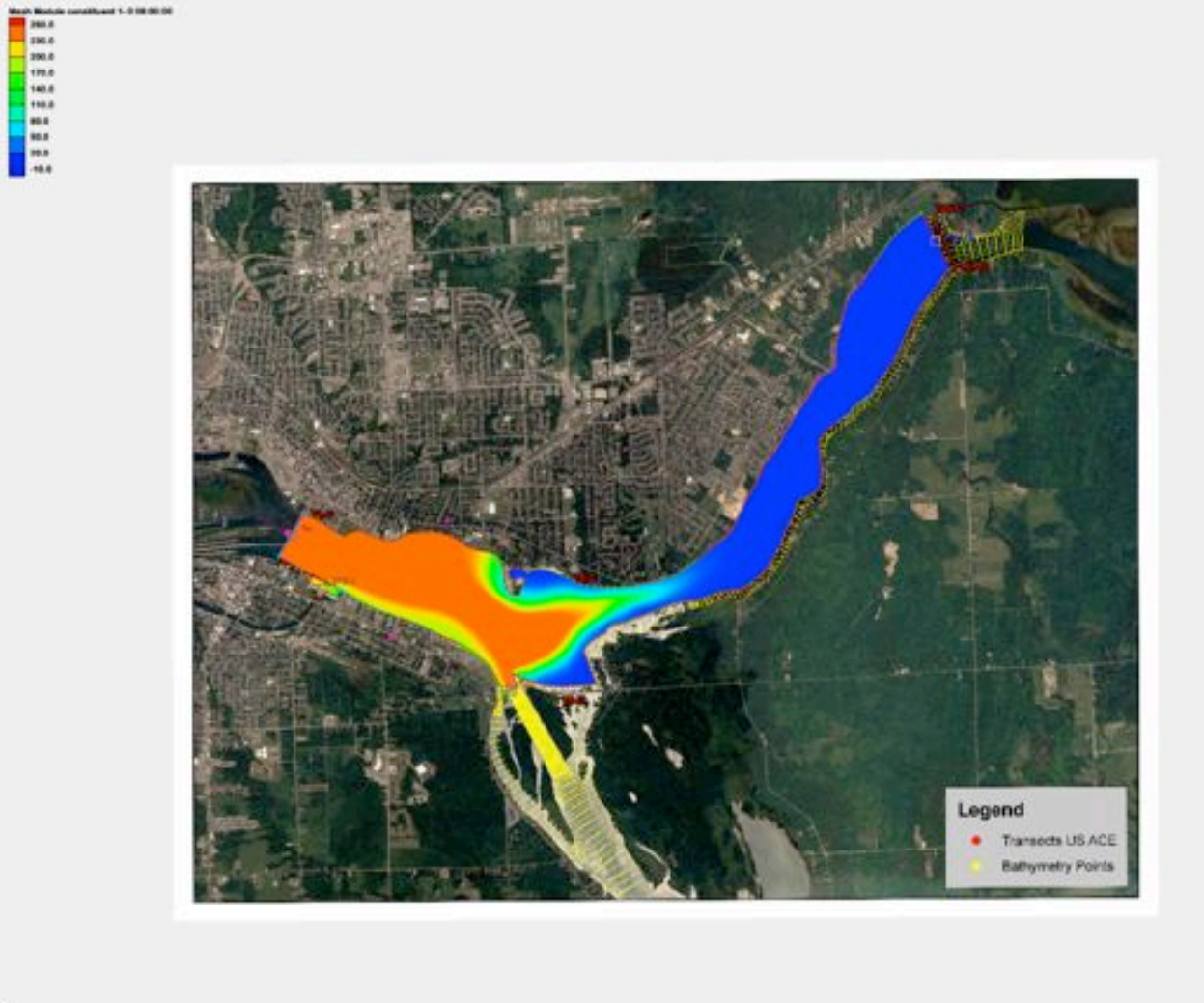

Fig. C4. Simulation of sediment transport in St. Marys River under low flow condition: Elapsed time = 8.0 hrs.

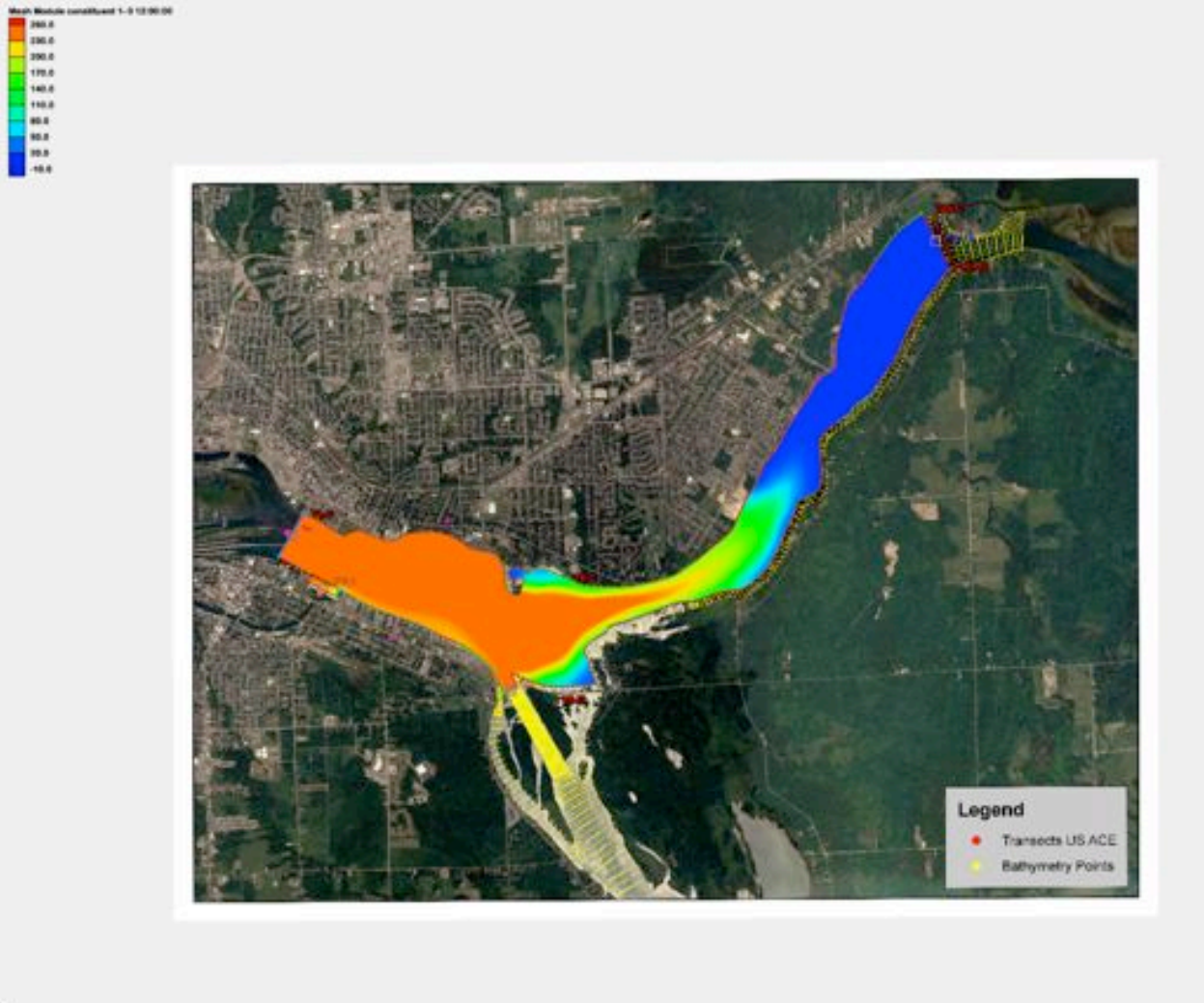

Fig. C5. Simulation of sediment transport in St. Marys River under low flow condition: Elapsed time = 12.0 hrs.

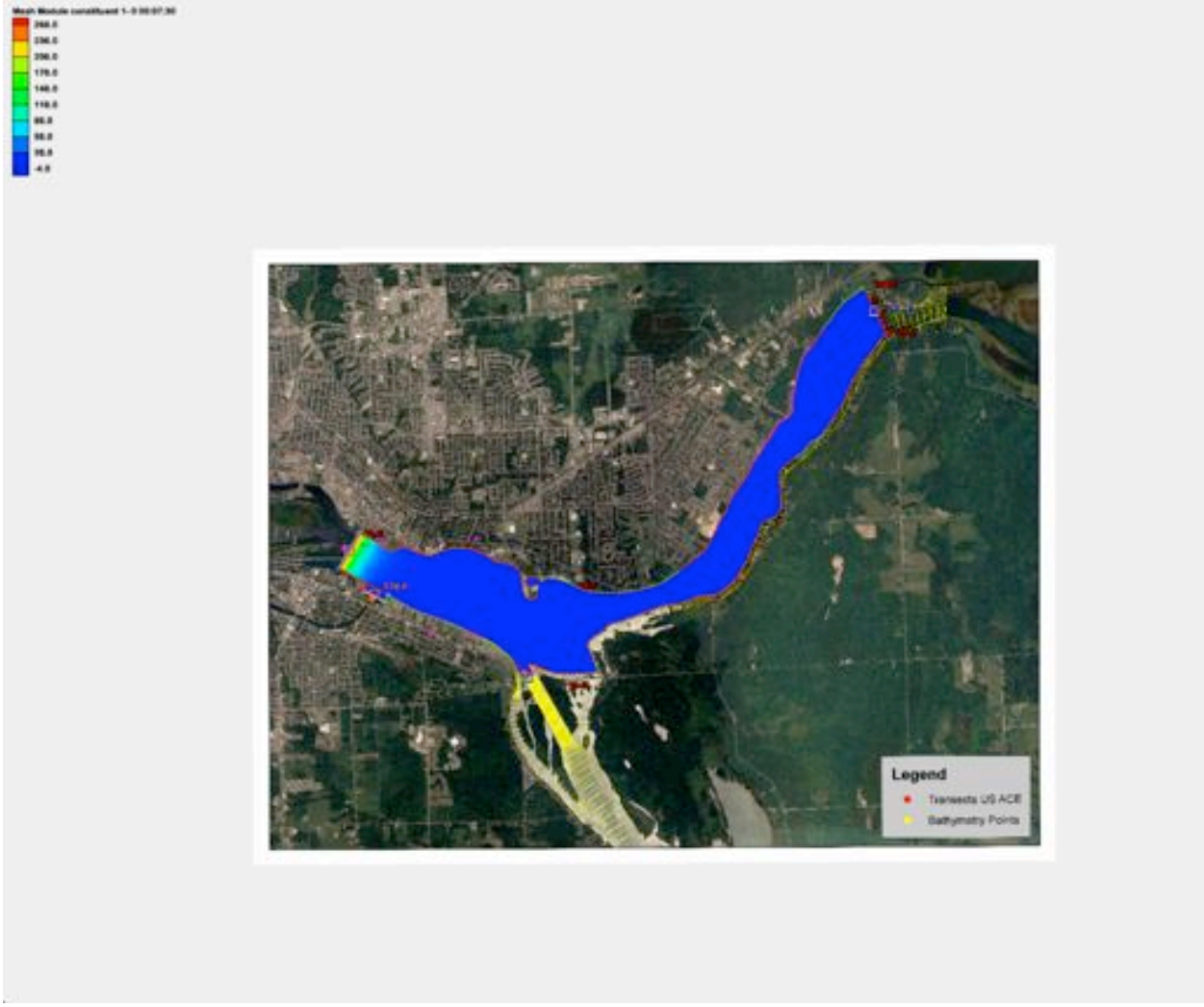

Fig. C6. Simulation of sediment transport in St. Marys River under high flow condition: Elapsed time = 0.125 hrs.

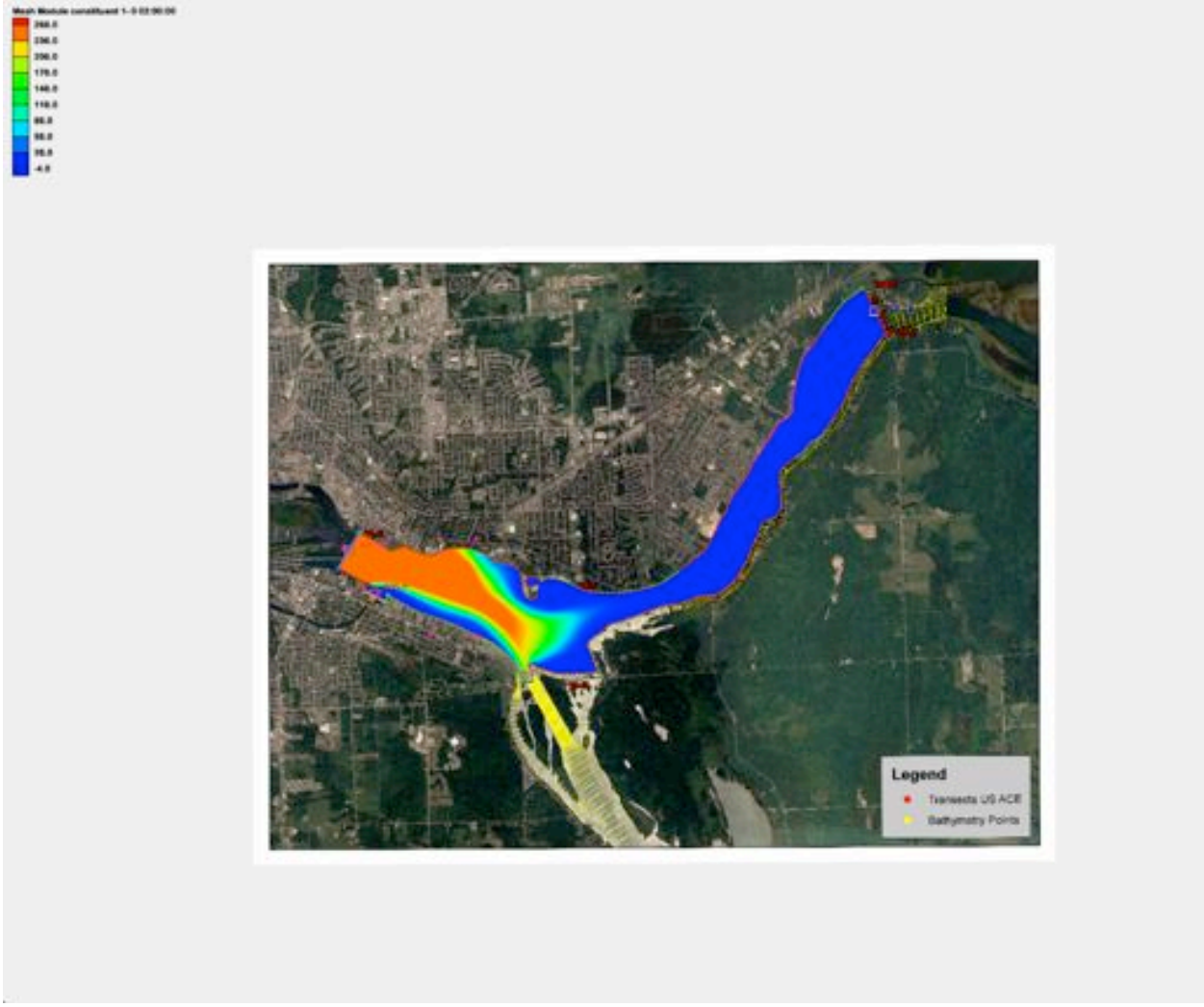

Fig. C7. Simulation of sediment transport in St. Marys River under high flow condition: Elapsed time = 2.0 hrs.

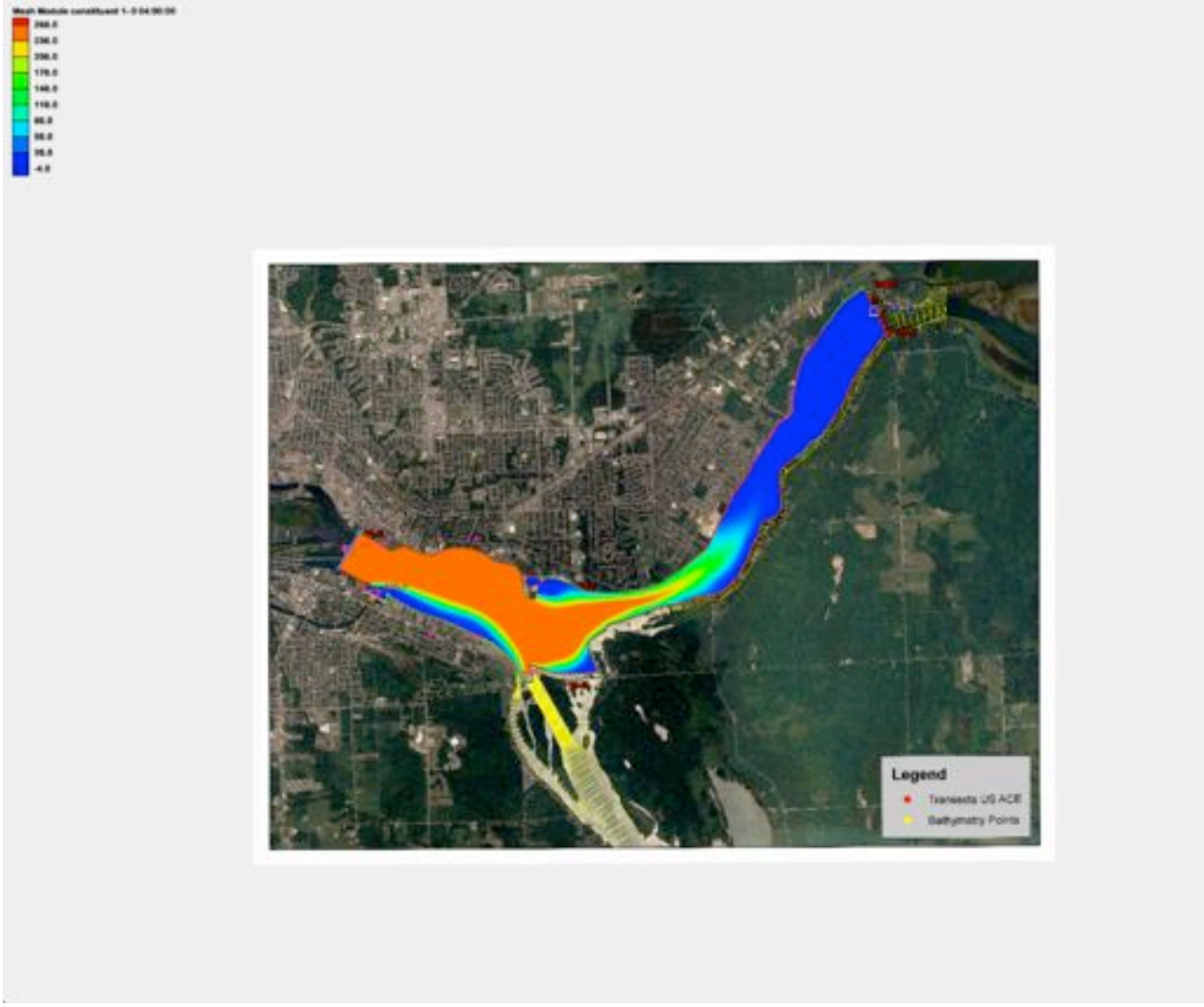

Fig. C8. Simulation of sediment transport in St. Marys River under high flow condition: Elapsed time = 4.0 hrs.

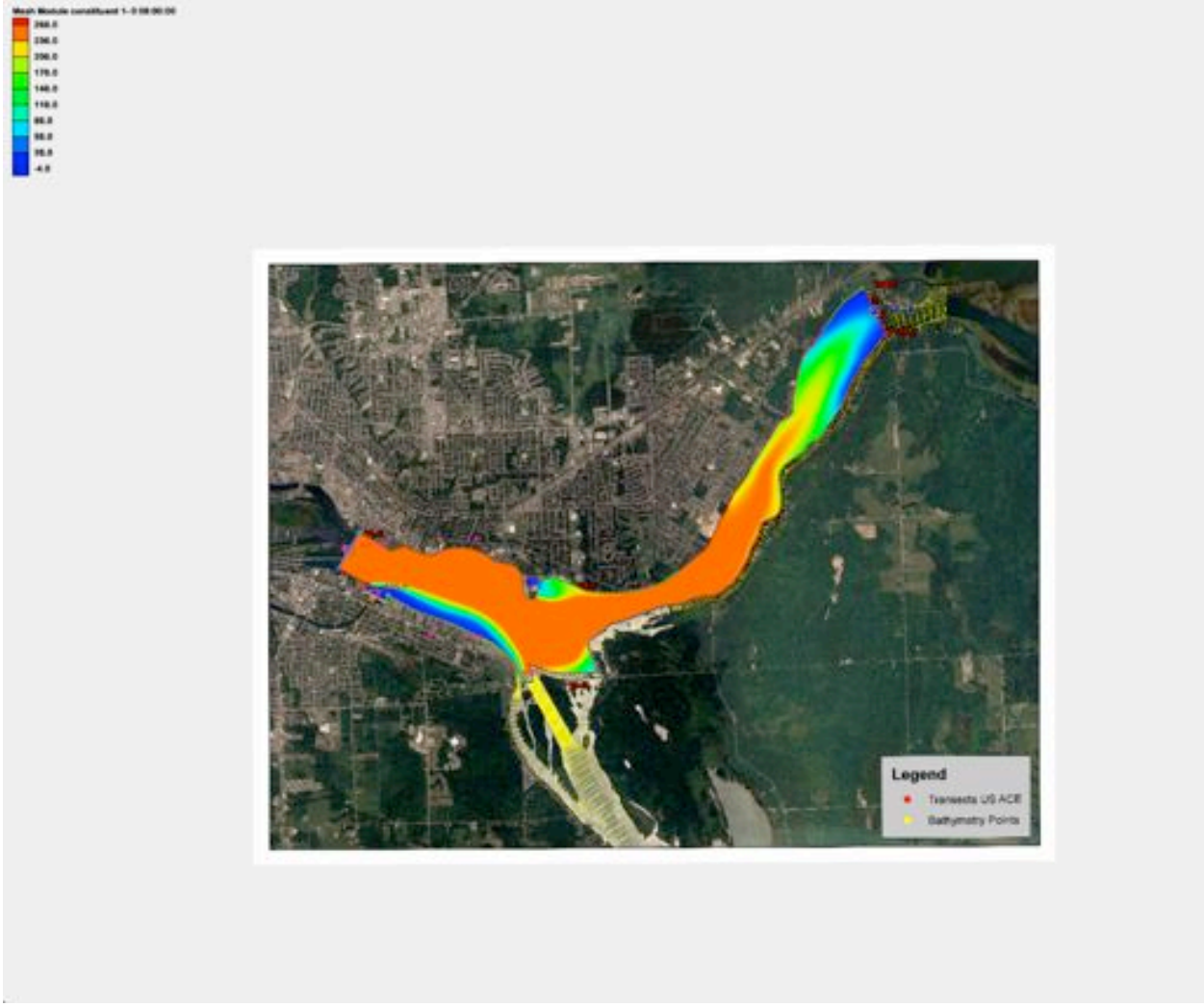

Fig. C9. Simulation of sediment transport in St. Marys River under high flow condition: Elapsed time = 8.0 hrs.

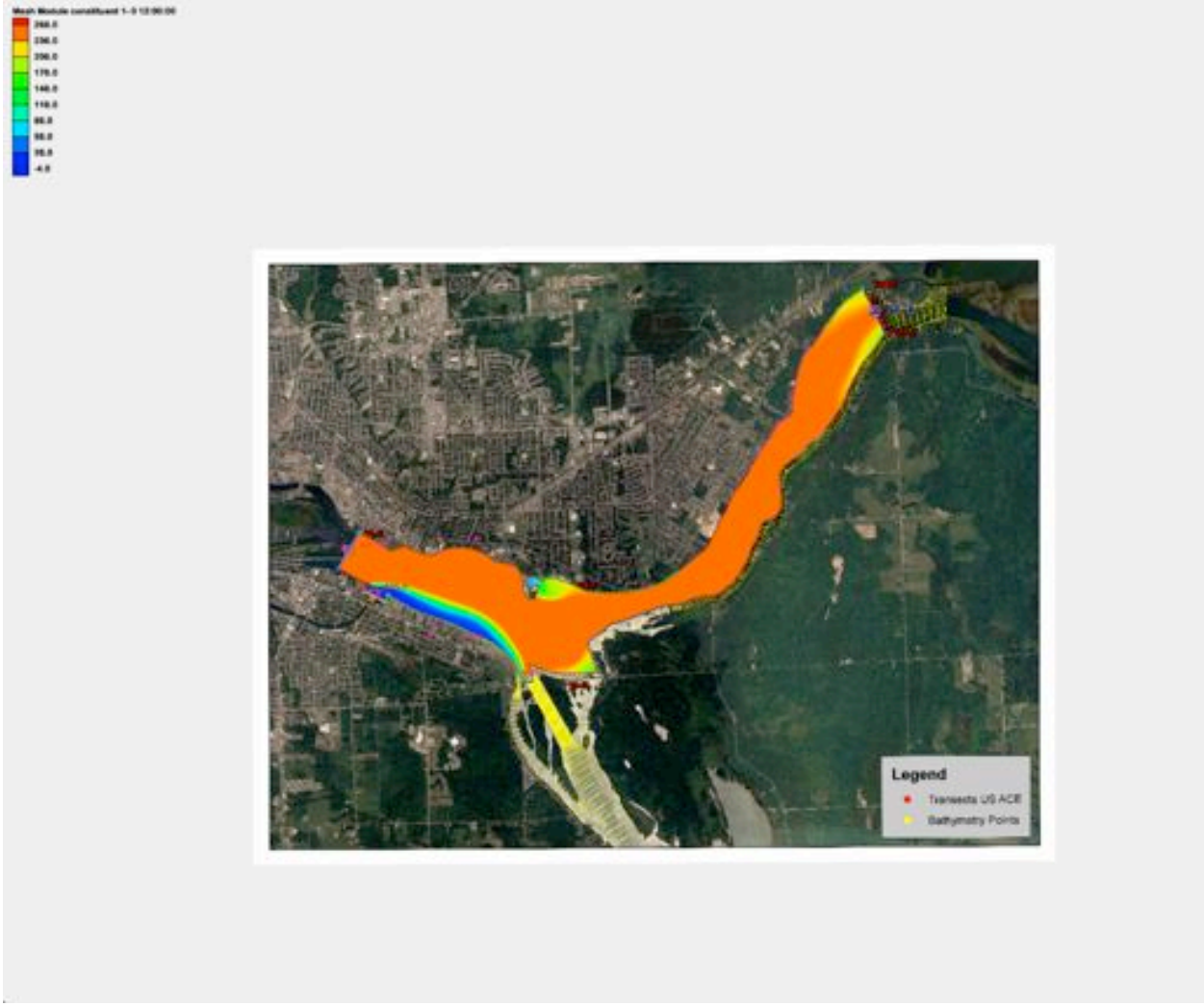

Fig. C10. Simulation of sediment transport in St. Marys River under high flow condition: Elapsed time = 12.0 hrs.